

NMR study of AgInTe_2 at normal and high pressure

Robin Guehne,^{*,†} Carsten Kattinger,[†] Marko Bertmer,[†] Simon Welzmler,[‡]
Oliver Oeckler,[‡] and Jürgen Haase[†]

[†]*Felix Bloch Institute for Solid State Physics, Leipzig University, Linnéstraße 5, 04103
Leipzig, Germany*

[‡]*Institute for Mineralogy, Crystallography and Materials Science, Faculty of Chemistry and
Mineralogy, Leipzig University, Scharnhorststr. 20, 04275 Leipzig, Germany*

E-mail: r.guehne@physik.uni-leipzig.de

Abstract

The ternary semiconductor AgInTe_2 is a thermoelectric material with chalcopyrite-type structure that transforms reversibly into a rocksalt-type structure under high pressure. Nuclear magnetic resonance (NMR) is considered to provide unique insight into material properties on interatomic length scales, especially in the context of structural phase transitions. Here, ^{115}In and ^{125}Te NMR is used to study AgInTe_2 for ambient conditions and pressures up to 5 GPa. Magnetic field dependent and magic angle spinning (MAS) experiments of ^{125}Te prove strongly enhanced internuclear couplings, as well as a distribution of isotropic chemical shifts suggesting a certain degree of cation disorder. The indirect nuclear coupling is smaller for ^{115}In , as well as the chemical shift distribution in agreement with the crystal structure. The ^{115}In NMR is further governed by a small quadrupolar interaction ($\nu_Q \approx 90$ kHz) and shows an orders of magnitude faster nuclear relaxation in comparison to that of ^{125}Te . At a pressure of about 3 GPa, the ^{115}In quadrupole interaction increases sharply to about 2400 kHz, indicating a phase transition to a structure with a well defined, though non-cubic local symmetry, while the ^{115}In shift suggests no significant changes of the electronic structure. The NMR signal is lost above about 5 GPa (at least up to about 10 GPa). However, upon releasing the pressure a signal is recovered that points to the reported metastable ambient pressure phase with a high degree of disorder.

Introduction

The ternary chalcogenide AgInTe_2 is of particular interest as a stoichiometric thermoelectric material for its ability to form solid solutions, e.g. $\text{AgIn}_x\text{Sb}_{1-x}\text{Te}_2$,¹ with a wide range of energy band gaps and lattice parameters.²⁻⁴ AgInTe_2 is also known to undergo a structural phase transition from its 4-fold coordinated chalcopyrite-type crystal structure ($I\bar{4}2d$, cf. Fig. 3a inset) at ambient conditions to a 6-fold coordinated NaCl-type structure (or possibly a slightly distorted variant thereof) with cation disorder between 3 and 4 GPa.⁵⁻⁸ Upon

decompression, it has been reported to form a metastable sphalerite-type structure with cation disorder.⁶

Nuclear magnetic resonance (NMR) studies of this type of material are not known, although, they should provide insight into properties of the various phases from a local probe’s perspective. NMR studies of related compounds such as InP date back several years – focusing on chemical properties like bonding character^{9–11} and nuclear exchange interactions^{12–18} – but do not include AgInTe₂.

We became interested in this material because of the intriguing behavior under pressure, given our recent endeavor into high pressure NMR studies of solids with anvil cells that currently allow studies under up to about 10 GPa (100 kbar) of pressure.^{19–21} In order to obtain a high sensitivity with the associated small sample that fits the pressure cell, we use radio-frequency (RF) microcoils inside the pressurized region (for a description of the setup see also Fig. S2 of the Supplementary Information (SI)). In fact, a first application with AgInTe₂ appeared to show an insulator-to-metal transition²² that we wanted to revisit.

Here we report on a more comprehensive ¹¹⁵In and ¹²⁵Te NMR study of AgInTe₂ at ambient and high pressure. With field dependent, MAS, and high pressure NMR we characterize both, chemical properties of the ambient condition phase as well as the structural phase transitions upon pressurization and subsequent pressure relief.

Methods

AgInTe₂ was prepared by melting stoichiometric amounts of elements Ag (99.999 %, Premion), In (99.999 %), and Te (puriss., both from VEB Spurenmittel Freiberg) in a sealed silica ampule under dry Ar atmosphere. After fusing the starting materials at 950 °C, the ampule was quickly cooled in air, followed by annealing at 400 °C. The ingots obtained showed gray metallic luster. For the NMR experiments a fine powder was used.

A powder X-ray diffraction pattern (cf. Fig. S1 in SI) of a representative part of the

sample fixed on a specimen holder with Mylar foil was recorded using a Huber G670 Guinier diffractometer with fixed imaging-plate detector and automatic read-out system (Cu-K $_{\alpha 1}$ radiation, Ge(111) monochromator, $\lambda = 1.54056 \text{ \AA}$). It showed no impurity, and homogeneity was also confirmed by a Rietveld fit based on a chalcopyrite-type structure model.

NMR experiments were carried out at static magnetic fields of 2.35 T, 7 T, 9.4 T, 11.7 T, and 17.6 T, as well as with a variable field magnet of up to 16 T, using commercial Bruker or Tecmag NMR consoles. Home-built, cryogenic (5 to $\sim 400 \text{ K}$), as well as commercial MAS probes (Bruker) with 4 mm rotors were employed. The sample container and the radio frequency (RF) coil were individually optimized for the experiment to allow best excitation conditions and filling factors, except for MAS applications.

We investigated mainly the ^{115}In nucleus, and obtained some results for ^{125}Te . Single pulse excitation was used to measure the free induction decay (FID) for sufficiently narrow resonance lines or MAS experiments. Spin echo pulse sequences ($\pi/2 - \tau - \pi$) were employed to measure broad spectra selectively, as well as transverse relaxation (T_2) with different pulse lengths and at different RF power levels. Solid echoes ($\pi/2 - \tau - \pi/2$) were employed to excite broad spectra non-selectively. Saturation ($\pi/2 - \tau_1$ -FID/spin echo) and inversion ($\pi - \tau_1$ -FID/spin echo) recovery pulse sequences were used to measure the spin-lattice relaxation ($1/T_1$).

For ^{115}In , the shift is referenced with respect to $\text{In}(\text{NO}_3)_3$, while for ^{125}Te , the shift is referenced to $\text{Te}(\text{CH}_3)_2$ (determined by the secondary reference method and metallic copper²³).

High Pressure Experiments: Home-built titanium body anvil cells^{19,24} were used for high pressure experiments up to 5 GPa (50 kbar) of pressure (the signal was lost at higher pressure). RF microcoils with diameters between 200 μm and 450 μm using insulated silver wire (Goodfellow Cambridge Ltd) with a diameter of 25 μm (5 μm insulation) were placed inside the sample chamber (cf. SI). Small amounts of the powder sample were placed within

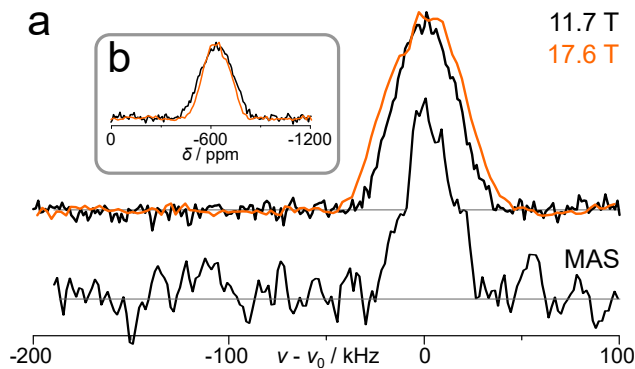


Figure 1: ^{125}Te NMR spectra at two different field strengths, 11.7 (black) and 17.6 T (orange), on the frequency (a) and ppm (b) scale. The MAS (12 kHz) spectrum (bottom) was recorded at 11.7 T and shows hardly any narrowing (no spinning sidebands are seen) when compared to the static spin echo FT spectrum above; at 17.6 T the signal broadens only slightly, as the corresponding spectra in (b) show (the spectra in units of ppm are given with respect to $\text{Te}(\text{CH}_3)_2$). For the static measurements we averaged 24 spin echoes with $\pi/2$ pulse lengths of $1.5 \mu\text{s}$ and a delay of $\tau = 45 \mu\text{s}$. For MAS experiments, 4 single pulse FIDs were averaged with $10 \mu\text{s}$ pulse length.

the coil region together with ruby chips for pressure monitoring (optical R1 and R2 line luminescence after laser excitation²⁵). Typical quality factors (Q) of such cells range between 10 to 30 which corresponds to bandwidths of about 3.5 to 11 MHz for a ^{115}In resonance frequency close to 110 MHz at 11.7 T.

Results

Ambient pressure

We show ^{125}Te NMR spectra (spin 1/2, $\gamma = 13.545 \text{ MHz/T}$, abundance of about 7%) in Fig. 1. The observed chemical shift of -630 ppm points to Te^{2-} ,²⁶ but we note a significant linewidth of about 250 ppm (39 kHz at 11.7 T), which does not narrow under sample spinning. Furthermore, the resonance must have a significant field-independent contribution as the linewidth slightly decreases on the ppm scale by going to higher field, cf. Fig. 1b. The spin echo decay is rather fast and Gaussian at the beginning, with an approximate $T_{2G} \approx 180 \mu\text{s}$ (Fig. S3 in SI), while the spin-lattice relaxation time T_1 is found to be about 360 s.

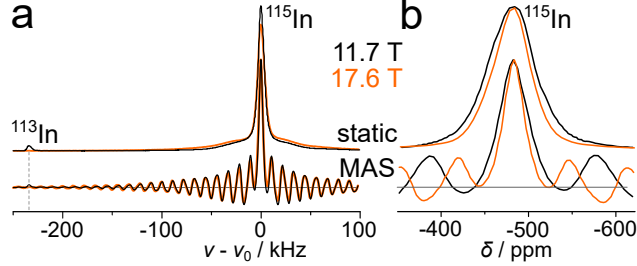


Figure 2: ^{115}In NMR spectra at two different magnetic fields with and without MAS (10 kHz) on (a) a large frequency range, and (b), the narrow line on the ppm scale. While the central line narrows moderately under rapid spinning, the broad line shows a large number of spinning sidebands. One notes significant field independent contributions to the linewidths. The resonance of the ^{113}In nucleus can be seen in (a) at -235 kHz. The shift is measured with respect to $\text{In}(\text{NO}_3)_3$.

The ^{115}In NMR spectra (spin $9/2$, $\gamma = 9.3857$ MHz/T, abundance of about 95%) are shown in Fig. 2. The narrow, symmetric peak shows a chemical shift of about -481 ppm with a linewidth of only 62 ppm (~ 7 kHz at 11.7 T). The slight deviation of the local symmetry from a perfect cubic environment (cf. inset of Fig. 3a) results in a small quadrupole interaction leading to a narrow central transition and a broad resonance given by the orientation dependent satellite transitions of the powder. Such a satellite distribution is known to average very well under MAS as found in the experiment. The spin echo decay is about $90 \mu\text{s}$, though, not a single exponential, and the spin-lattice relaxation is about a factor of 10^4 faster (30 ms) than that of Te, again pointing to the importance of quadrupole interaction for the ^{115}In nucleus ($eQ \approx 77.2(5) \times 10^{-30} |\text{e}| \text{m}^{-2}$).

In order to better resolve the ^{115}In NMR signal, we recorded the total spectrum with frequency stepped, selective spin echoes, as well as broad band quadrupole echoes.²⁷ For the spin echoes we used a probe with a high Q, and long pulses (low power) were employed to ensure selective excitation. A typical spectrum is shown in Fig. 3a. While the broad peak is much better visible, it does not show singularities typical for powder spectra. Nevertheless, the shape of the broad line with a quite separate and narrow central transition points to a quadrupole tensor with some asymmetry. We can fit the total spectrum with a quadrupole first-order spectrum with $\nu_Q = 90$ kHz, $\eta = 0.3$, and an additional broadening of 7 kHz.

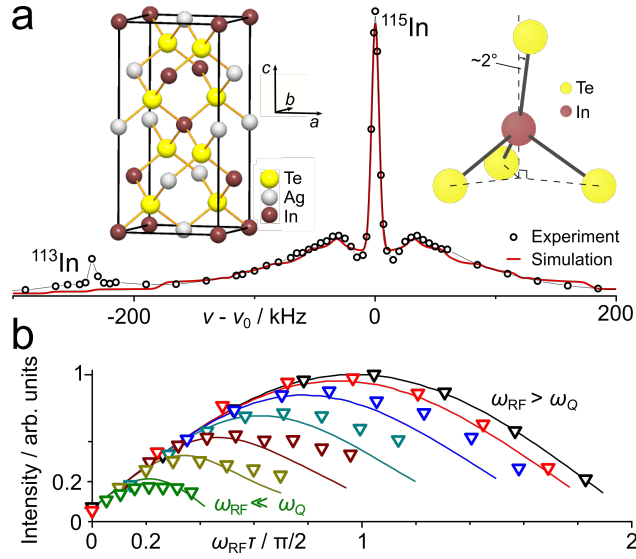


Figure 3: **(a)** combined selective spin echoes ($\pi/2$ pulse width $50 \mu\text{s}$) of ^{115}In and ^{113}In nuclei obtained at 11.7 T shown as circles. The red solid line represents a first-order quadrupole powder simulation (see text for details). The inset on the left shows the crystal structure of AgInTe_2 , and on the right, the arrangement of the 4 Te atoms surrounding In as obtained from Rietveld refinement (cf. SI). **(b)** nutation experiments of the ^{115}In central transition (triangles) at different power levels from non-selective excitation with $\omega_{\text{RF}}/\omega_{\text{Q}} \approx 4.3$ (black) to selective excitation with $\omega_{\text{RF}}/\omega_{\text{Q}} \approx 0.077$ (green). Solid lines represent simulations for various excitation power levels ω_{RF} .

Nutation experiments measured of the central transition with a low-Q probe reveal that the broad line is indeed caused by the estimated quadrupole interaction.

Finally, we show in Fig. 4 the results of ^{115}In and ^{125}Te relaxation measurements, including a temperature dependence of the ^{115}In spin-lattice relaxation rate that verifies the interaction with phonons to be the main cause. Also shown are the field dependences of the linewidths of ^{115}In and ^{125}Te to determine possible field-independent contributions. The results are discussed below.

Elevated pressure

As described under *Methods*, NMR anvil cells with RF microcoils were used for these experiments. The very small coil volume and the inherently low Q of the coils warrant high time resolution, but also limit the signal-to-noise. Therefore, we only report on the ^{115}In

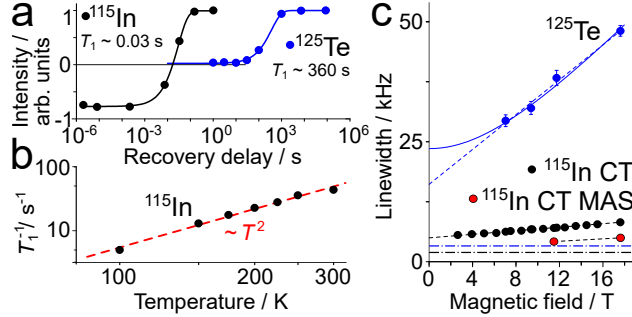


Figure 4: (a) spin-lattice relaxation measurements of ^{115}In (black, non-selective excitation, inversion recovery) and ^{125}Te nuclei (blue, saturation recovery). In panel (b) we show the ^{115}In relaxation rate as a function of temperature in a log-log plot together with a T^2 dependence (red dashed line). (c) the static and 10 kHz MAS linewidths (full width at half maximum) of the ^{115}In CT (black and red, respectively), as well as for ^{125}Te (blue) as functions of the external magnetic field. Dashed lines represent best fits to linear dependences and the solid line a $(\Lambda^2 = \Lambda_0^2 + (bB_0)^2)$ relationship between linewidth and field. The dash-dotted lines at the bottom denote the calculated line broadening from direct dipole-dipole interactions for ^{115}In (2 kHz) and ^{125}Te (3.3 kHz) using the method of moments.²⁸

resonance, mostly recorded after non-selective quadrupole echo excitation.²⁷ The results are summarized in Fig. 5.

At ambient pressure (Fig. 5a) we obtain within error the same spectrum as in Fig. 3a. The change of shape of the broad foot as the pressure increases to 1.4 and 2.5 GPa is due to an increase in the quadrupole frequency, which is proven with the nutation experiments shown in panel (b). At 3 GPa, the narrow signal is nearly lost, and replaced by a second-order central line quadrupole powder pattern (red shaded area), while some portion of the nuclear spins seem still to be subject to a smaller quadrupole interaction as they form the rather narrow peak in the middle of the spectrum. At 4 GPa, the second-order quadrupole spectrum is much better resolved. A fit with a $\nu_Q = 2420$ kHz and $\eta = 0.18$ is shown (the same as used for the red shaded area in the 3 GPa spectrum). Unfortunately, above 5 GPa we lost the NMR signal. Then we released the pressure and measured again at ambient condition to find the spectra (solid echo FT) shown at the bottom in panel (a) (acquired about two weeks (*) and eight months (**)) after decompression). We find a resonance line at the ambient pressure shift but with a much larger linewidth of about 50 kHz.

The chemical shift of the central transition as a function of pressure shows a significant

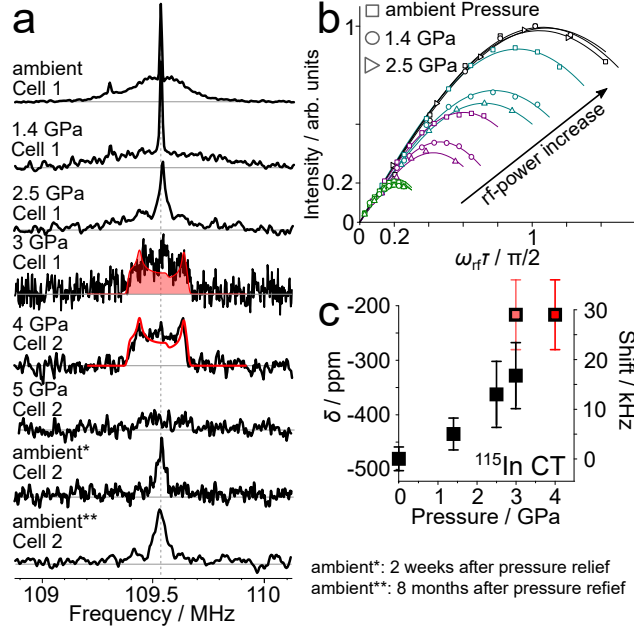


Figure 5: (a) Spectra at various pressures including ambient pressure after pressure relief ((*) and (**)) at the bottom of the panel. Quadrupole echoes ($0.5\mu\text{s}$ $\pi/2$ pulses) were used for recording, except for the spectra at 4 GPa and 5 GPa, for which spin echo sequences with $0.5 - 1.0\mu\text{s}$ were used. Spectra were normalized since the signal-to-noise varied. The red shaded area in the 3 GPa spectrum represents a second-order quadrupole simulation as obtained from the 4 GPa spectrum (red solid line, see text for details). (b) nutation experiments (colored symbols) for ambient, 1.4 and 2.5 GPa pressure confirm a moderate increase of the quadrupole interaction with increasing pressure. Data points with the same color denote the same excitation power levels. Solid lines are guides to the eye. (c) magnetic shift of the central transition as a function of pressure, in ppm with respect to $\text{In}(\text{NO}_3)_3$, and in kHz with respect to the ambient pressure resonance frequency. The 3 and 4 GPa values (red data point) are corrected for the second-order quadrupole shift.

increase (from -481 to about -220 ppm), but not such a sudden change as for the quadrupole interaction.

Discussion

Ambient pressure

The rather long ^{125}Te (spin-1/2) spin-lattice relaxation time, $T_1 \approx 6$ min, is perhaps expected for this semiconducting material with a sizable bandgap and shows that magnetic excitations are largely absent. The negative shift is expected for a Te^{2-} ion, but the large ^{125}Te NMR

linewidth (≈ 250 ppm) points to disorder in the Te environment. A certain degree of disorder in the Ag and In distribution, which cannot be elucidated in a straightforward way by X-ray crystallography due to the lacking scattering contrast, is a likely explanation. For example, if Te has 3 In and 1 Ag as nearest neighbors (instead of 2 In and 2 Ag), the tetrahedral environment will be more strongly distorted, which likely affects more the isotropic shift. Four In or 4 Ag neighbors would result in different isotropic shifts. Therefore, such disorder, if abundant, should contribute to the linewidth. And since we detect roughly all ^{125}Te nuclei, this would explain the observed shift variation and the rather Gaussian lineshape that does not narrow under MAS. For a more quantitative study, compounds with Ag_3In and AgIn_3 environments for Te would be desirable, as well as first principle calculations. The spin echo decay of ^{125}Te is Gaussian at the beginning and is likely to be given by the $^{125}\text{Te} - ^{125}\text{Te}$ homonuclear interaction. The strong field independent linewidth (up to about 25 kHz, cf. Fig. 4c) points to a large internuclear coupling (J -coupling) predominately between ^{125}Te nuclei and their ^{115}In neighbors, which can also contribute to the linewidth under MAS. Such enhanced internuclear interactions involving heavy element nuclei have also been reported for related semiconductors.^{12–18}

The nuclear relaxation of ^{115}In is about 4 orders of magnitude faster than that of ^{125}Te . Since of the gyromagnetic ratios ($^{115}\gamma/^{125}\gamma \approx 0.69$) cannot account for such a difference in T_1 , this points to a strong quadrupolar mechanism. The ^{115}In T_1 temperature dependence shown in Fig. 3b (quadratic in temperature above half of the Debye temperature, $\theta_D = 202 \text{ K}$ ²⁹) documents that Raman processes involving all phonons cause the observed behavior.^{30,31} It might even be possible to relate the relaxation rate to the actual density of states of the phonons if one could compare with corresponding data on different systems. The observed quadrupole splitting due to the slightly distorted tetrahedral environment is not well resolved and the linewidths vary slightly between the frequency stepped spin echo data and the Fourier transform of quadrupole echoes (with long pulse delays to suppress the influence of Solomon echoes²⁷). Also, one notices the absence of any singularities often found with powder patterns.

This points to distributions of the tensor components of the electric field gradient, but given the mentioned uncertainties we did not attempt to pursue particular fits. We estimate a quadrupole frequency of about 90 kHz with an asymmetry parameter $\eta \approx 0.3$.

The ^{115}In NMR line at about -480 ppm has a linewidth of about 62 ppm that narrows under MAS to about 28 ppm (~ 3 kHz). As Fig. 4c shows, the field dependent contributions to the ^{115}In linewidth are much smaller than for ^{125}Te . This is expected since all ^{115}In neighbors are Te atoms, so that a somewhat random occupation of the cation sites is less important. Due to the low abundance of ^{125}Te , the local field at ^{115}In is mostly given by other In nuclei in the second shell (Ag has low- γ nuclei and does not contribute significantly). Therefore, the indirect coupling that contributes to the field independent linewidth (about 5 kHz) is expected to be much weaker at ^{115}In , as well. The spin echo decays can be found in the SI.

Pressure dependence

The dependence of the quadrupole coupling on pressure is interesting. After a moderate change of the quadrupole splitting up to about 2.5 GPa, a sudden increase at 3.0 GPa follows. Importantly, this phase has a rather well-defined second-order quadrupole pattern, pointing to a more or less well ordered structure. Certainly, this finding disagrees with a cubic NaCl structure that was discussed in the literature, because cation disorder (second coordination sphere) is not expected to yield such a strong and well defined deformation of the local charge distribution. Rather, our data point at a crystal structure with a non-cubic In environment. Based on the diffraction of synchrotron radiation of AgInTe_2 for pressures up to 6.2 GPa, Bovornratanaraks et al. (2010) come to a similar conclusion.⁷ While they observe slight changes of the reflection patterns for low pressures and a gradual replacement of the ambient structure by the high pressure phase around 3 to 4 GPa (in good agreement with our quadrupole data), the authors question the consensus of a NaCl-type high pressure structure in favor of a cation-disordered $Cmcm$ phase, although XRD data remain ambiguous. Here, NMR provides additional evidence from a local perspective for such a crystal structure

with non-cubic ^{115}In environment. Aided by first principles calculations, the quadrupole frequency and the asymmetry parameter as obtained from the second-order quadrupole fit may be used to assess the local In environment of the high pressure phase in greater detail. Finally, the rather moderate changes of the chemical shift of about 150 ppm by going from the chalcopyrite-type to the high pressure structure do not support significant changes in the electronic structure and thus, the occurrence of a metallic phase.

Unfortunately, we lost the signal above 4 GPa. With various pressure cells we searched for signal in a broad range of frequencies up to about 10 GPa since we expected a metallic phase.²² Measurements after pressure relief, however, prove a proper functioning of the anvil cells and the loss of signal must therefore have physical reasons. What caused the disappearance of the signal cannot be said with certainty as these measurements are difficult and time consuming. Possible reasons are further broadening of the NMR signal or an increase in relaxation time.

After we released the pressure from one of the cells, we obtained a spectrum governed by a single, rather narrow peak at the ambient pressure resonance frequency (cf. Fig. 5 (a), bottom spectrum), which has not noticeably changed after about 8 months under ambient conditions (the better signal-to-noise ratio of the second measurement is due to a greater number of averaged scans). The broadening of this resonance line (~ 50 kHz), however, is much larger in comparison to the initial linewidth for ambient pressure and the spectra may thus represent the metastable phase with zincblende-type structure ($\text{AgInTe}_2\text{-III}$) and randomly distributed cations.^{5,6}

The high pressure NMR data prove that the various stages of the phase transitions in a material like AgInTe_2 under the application of external pressure can clearly be distinguished, and using an optimized high pressure setup in combination with first principles calculations, structural as well as electronic properties could be studied with local resolution and high accuracy.

Conclusions

We investigated the ^{115}In and ^{125}Te NMR of powdered AgInTe_2 at ambient and ^{115}In NMR at high pressures. The ^{125}Te linewidth, studied for various fields and under MAS, suggests strongly enhanced internuclear interactions, as well as a distribution of isotropic shifts, yielding a large field independent linewidth and weak narrowing under MAS. Both features hold for the ^{115}In nuclei, though less pronounced, in agreement with a more symmetric local In environment. The internuclear coupling very likely causes the rather rapid and complex transverse relaxation phenomenology observed for both nuclei. Furthermore, ^{115}In nuclei are subject to a small quadrupole interaction of about 90 kHz and feature a quadrupolar spin-lattice relaxation orders of magnitude faster compared to that of ^{125}Te nuclei. With increasing pressure, the quadrupole interaction increases moderately at the beginning, but sharply around 3 GPa to about 2400 kHz. This indicates a phase transition to a rather well ordered structure with lowered local symmetry, in agreement with literature data. The shift increases almost continuously from about -500 to -200 in the same pressure range, implying no significant electronic changes. Above about 5 GPa, the NMR signal is lost and could not be found up to about 10 GPa. Upon decompression, however, we recovered a resonance line with the same shift but a much bigger linewidth as the initial ambient spectrum. The line broadening may be due to the reported⁶ metastable sphalerite-type structure with random cation distribution.

Supporting Information

Powder X-ray diffraction and Rietveld refinement

A Huber G670 Guinier camera equipped with a fixed imaging-plate and an automatic read-out system ($\text{CuK}_{\alpha 1}$ radiation, Ge(111) monochromator, $\lambda = 1.54056 \text{ \AA}$) was used to record the powder X-ray diffraction patterns of the investigated sample to quantify sample homogeneity

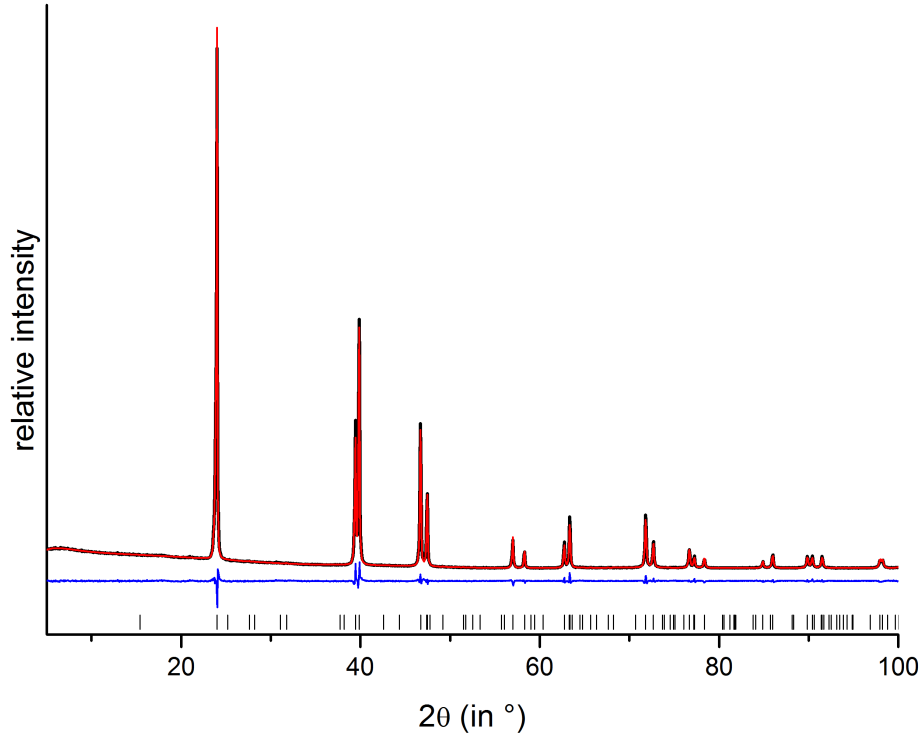


Figure 6: Black, powder XRD reflection pattern of AgInTe_2 as measured, in Red, results from the Rietveld refinement, and in Blue, the difference plot. Rietveld refinement confirms space group $I\bar{4}2d$ and determines $a = 6.45741(6)$ and $c = 12.65146(17)$.

and lattice parameters. To fix representative parts of the powdered sample on a specimen holder with Mylar foil, hair-fixing spray was used.

Using Topas Academic software, Rietveld and Pawley fits were carried out. The reflection profiles were described with a direct convolution approach and fundamental parameters. The emission profile was described using a Pseudo-Voigt function.

Table 1: Rietveld refinement details

| R_p | R_{wp} | R_{wp}^* | R_{Bragg} | χ^2 |
|--------|----------|------------|-------------|----------|
| 0.0177 | 0.0277 | 0.0834 | 0.0169 | 1.232 |

*background subtracted

High-pressure NMR setup

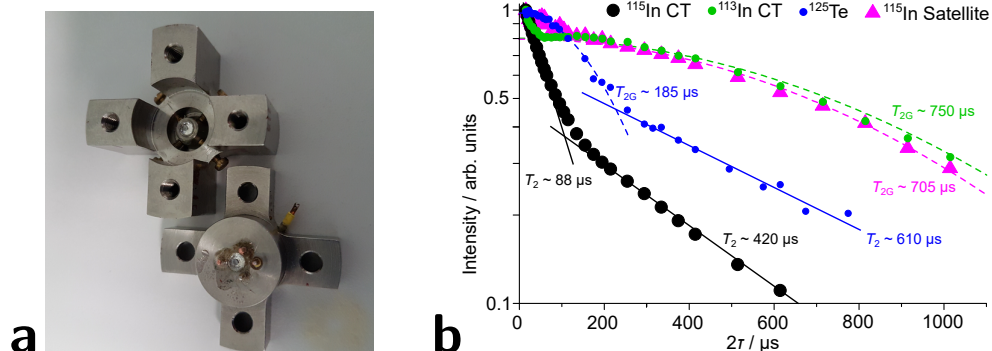


Figure 7: High pressure NMR setup. (a) The open titanium cell as used in high pressure experiments, with the two Moissanite visible in the middle of the two cell halves. In the closed cell, the tips (culets) of the two anvils enclose the sample chamber as depicted in panel (b), containing the NMR microcoil with the sample, ruby chips for pressure monitoring, as well as a pressure medium (paraffin oil) to ensure hydrostatic conditions. A non-magnetic CuBe gasket keeps the arrangement in place.

Transverse relaxation measurements

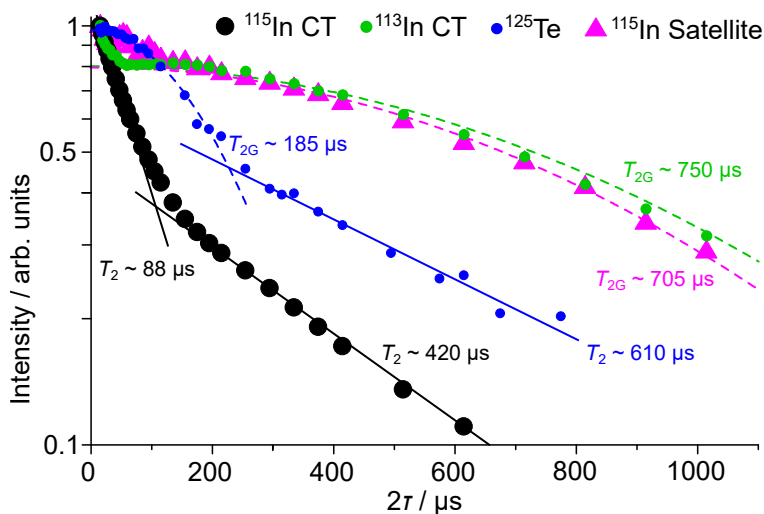


Figure 8: Spin echo decay measurements obtained for various resonances. All measurements were carried out under selective excitation conditions. ^{115}In satellite' represents a narrow slice in the quadrupole powder spectrum about 150 kHz above the central transition where it was ensured that the latter is not excited during the measurement. Solid lines represent single exponential decays (T_2), while dashed lines assume Gaussian decays (T_{2G}).

In Fig.8, we present the spin echo decays observed for both In nuclei and Te. The decay of the selectively excited central transition for ^{115}In is very fast ($T_2 \approx 88 \mu\text{s}$) at the beginning before the slope changes to a much slower decay with $T_2 \approx 420 \mu\text{s}$. Both decays are well approximated with a single exponential. Similar experiments on the satellites give even larger values of $T_{2G} \approx 705 \mu\text{s}$, while the shape of the decay is Gaussian-like. This means, the spin flips allowed for the central levels (not affected by the quadrupole interaction) must be rather effective, while being quenched in the satellites³². This is also borne out by the ^{113}In NMR measurements. This low abundance nucleus has essentially ^{115}In neighbors due to the low abundance of ^{125}Te and the negligible Ag magnetic moments, and we further can neglect any like-spin interactions. It thus measures the local field fluctuations from surrounding ^{115}In spins, part of which will be in the central levels and show rapid spin exchange, for others it will be quenched. As a consequence we observe a two component decay also for the ^{113}In CT, for which the rapid decay stems from the effective homonuclear interaction that affects a refocussing of the second pulse. For ^{125}Te , as expected, we find a similar behavior with a rather fast, Gaussian spin echo decay at the beginning followed by a slower decay for τ greater than about $125 \mu\text{s}$.

These spin echo decay data highlight the complexity of the present couplings among the various nuclear magnetic moments. Although we are not able to provide quantitative description of this behavior, the mere rapidness of the observed decays, e.g., about $90 \mu\text{s}$ and $185 \mu\text{s}$ for the ^{115}In CT and ^{125}Te , respectively, strongly hints at enhanced dipolar interactions. Such strong internuclear interactions would then explain the large field independent linewidths as well as the failure of MAS to lead to a significant narrowing in particular for ^{125}Te , cf. Fig.1 of the main manuscript. For ^{115}In the residual linewidth of 4 to 5 kHz is in agreement with the effective homonuclear decay of the central transition, Fig.4b in the main manuscript. Faster spinning should be more effective. However, we are also not certain whether the enhanced coupling is of pseudo dipolar origin and thus shows an angular dependence under rotation. It might as well be a result of an indirect nuclear coupling of the Bloembergen-Rowland type

with a fairly isotropic line broadening such that it would not be affected by MAS. If aided by first principle calculations, more information about the details for the structure could be readily obtained. Such enhanced internuclear interactions that involve electronic exchange couplings and yield effective line broadening even under MAS have already been reported for similar systems, namely for InP, InAs, and InSb^{12–18}.

Acknowledgement

We thank V. Chlan (Prague) for fruitful discussions and G. Klotzsche (Leipzig) for technical support. We acknowledge the financial support by the Deutsche Forschungsgemeinschaft, projects 317319632 and 442459148, and by Leipzig University.

References

- (1) Schröder, T.; Rosenthal, T.; Souchay, D.; Petermayer, C.; Grott, S.; Scheidt, E.-W.; Gold, C.; Scherer, W.; Oeckler, O. A high-pressure route to thermoelectrics with low thermal conductivity: The solid solution series $\text{AgIn}_x\text{Sb}_{1-x}\text{Te}_2$ ($x = 0.1\text{--}0.6$). *J. Solid State Chem.* **2013**, *206*, 20–26.
- (2) Kasiviswanathan, S.; Rao, D. K.; Gopalam, B. Preparation and characterization of the pseudobinary system $\text{Cu}_{1-x}\text{Ag}_x\text{InTe}_2$. *J. Mater. Sci. Lett.* **1986**, *5*, 912–914.
- (3) Welzmler, S.; Hennersdorf, F.; Fitch, A.; Oeckler, O. Solid solution series between CdIn_2Te_4 and AgInTe_2 investigated by resonant X-ray scattering. *Z. Anorg. Allg. Chem.* **2014**, *640*, 3135–3142.
- (4) Welzmler, S.; Hennersdorf, F.; Schlegel, R.; Fitch, A.; Wagner, G.; Oeckler, O. Silver Indium Telluride Semiconductors and Their Solid Solutions with Cadmium Indium Telluride: Structure and Physical Properties. *Inorg. Chem.* **2015**, *54*, 5745–5756, PMID: 26023890.

- (5) Range, K.-J.; Engert, G.; Weiss, A. High pressure transformations of ternary chalcogenides with chalcopyrite structure — I. Indium-containing compounds. *Solid State Commun.* **1969**, *7*, 1749–1752.
- (6) Range, K.-J.; Engert, G.; Weiss, A. AgInTe₂-III — eine metastabile Modifikation des AgInTe₂? *Z. Naturforsch. B* **1969**, *24*, 813–814.
- (7) Bovornratanaraks, T.; Kotmool, K.; Yoodee, K.; McMahon, M. I.; Ruffolo, D. High pressure structural studies of AgInTe₂. *J. Phys.: Conf. Ser.* **2010**, *215*, 012008.
- (8) Kotmool, K.; Bovornratanaraks, T.; Yoodee, K. Ab initio study of structural phase transformations and band gap of chalcopyrite phase in AgInTe₂ under high pressure. *Solid State Commun.* **2015**, *220*, 25–30.
- (9) Lütgemeier, H. Die chemische Verschiebung der Kernresonanzlinien in A^{III}B^V-Verbindungen. *Z. Naturforsch. A* **1964**, *19*, 1297–1300.
- (10) Becker, K.; Schäffgen, H. NMR chemical shifts in copper (I) chalcogen compounds. *Solid State Commun.* **1979**, *32*, 1107–1109.
- (11) Vanderah, T.; Nissan, R. ³¹P MAS NMR of a II–IV–V₂ chalcopyrite-type series. *J. Phys. Chem. Solids* **1988**, *49*, 1335–1338.
- (12) Shulman, R. G.; Wyluda, B. J.; Hrostowski, H. J. Nuclear Magnetic Resonance in Semiconductors. III. Exchange Broadening in GaAs and InAs. *Phys. Rev.* **1958**, *109*, 808–809.
- (13) Engelsberg, M.; Norberg, R. E. Nuclear Magnetic Resonance and Nuclear-Spin Dynamics in InP. *Phys. Rev. B* **1972**, *5*, 3395–3406.
- (14) Han, O. H.; Timken, H. K. C.; Oldfield, E. Solid-state “magic-angle” sample-spinning nuclear magnetic resonance spectroscopic study of group III–V (13–15) semiconductors. *J. Chem. Phys.* **1988**, *89*, 6046–6052.

- (15) Tomaselli, M.; deGraw, D.; Yarger, J. L.; Augustine, M. P.; Pines, A. Scalar and anisotropic J interactions in undoped InP: A triple-resonance NMR study. *Phys. Rev. B* **1998**, *58*, 8627–8633.
- (16) Adolphi, N. L.; Conradi, M. S.; Buhro, W. E. The ^{31}P NMR spectrum of InP. *J. Phys. Chem. Solids* **1992**, *53*, 1073–1074.
- (17) Iijima, T.; Hashi, K.; Goto, A.; Shimizu, T.; Ohki, S. Indirect nuclear spin–spin coupling in InP studied by CP/MAS NMR. *Physica B* **2004**, *346-347*, 476–478, Proceedings of the 7th International Symposium on Research in High Magnetic Fields.
- (18) Iijima, T.; Hashi, K.; Goto, A.; Shimizu, T.; Ohki, S. Anisotropic indirect nuclear spin–spin coupling in InP: ^{31}P CP NMR study under slow MAS condition. *Chem. Phys. Lett.* **2006**, *419*, 28–32.
- (19) Haase, J.; Goh, S. K.; Meissner, T.; Alireza, P. L.; Rybicki, D. High sensitivity nuclear magnetic resonance probe for anvil cell pressure experiments. *Rev. Sci. Instrum.* **2009**, *80*, 073905.
- (20) Meissner, T.; Goh, S. K.; Haase, J.; Richter, M.; Koepernik, K.; Eschrig, H. Nuclear magnetic resonance at up to 10.1 GPa pressure detects an electronic topological transition in aluminum metal. *J. Phys.: Condens. Matter* **2013**, *26*, 015501.
- (21) Kattinger, C.; Guehne, R.; Tsankov, S.; Jurkutat, M.; Erb, A.; Haase, J. Moissanite anvil cell single crystal NMR at pressures of up to 4.4 GPa. *Rev. Sci. Instrum.* **2021**, *92*, 113901.
- (22) Meier, T.; Reichardt, S.; Haase, J. High-sensitivity NMR beyond 200,000 atmospheres of pressure. *J. Magn. Reson.* **2015**, *257*, 39–44.
- (23) Harris, R. K.; Becker, E. D.; De Menezes, S. M. C.; Granger, P.; Hoffman, R. E.;

- Zilm, K. W. Further conventions for NMR shielding and chemical shifts (IUPAC recommendations 2008). *Mag. Res. Chem.* **2008**, *46*, 582–598.
- (24) Meissner, T.; Goh, S. K.; Haase, J.; Meier, B.; Rybicki, D.; Alireza, P. New Approach to High-Pressure Nuclear Magnetic Resonance with Anvil Cells. *J. Low Temp. Phys.* **2010**, *159*, 284.
- (25) Forman, R. A.; Piermarini, G. J.; Barnett, J. D.; Block, S. Pressure measurement made by the utilization of ruby sharp-line luminescence. *Science* **1972**, *176*, 284–285.
- (26) Ruiz-Morales, Y.; Schreckenbach, G.; Ziegler, T. Calculation of ^{125}Te Chemical Shifts Using Gauge-Including Atomic Orbitals and Density Functional Theory. *J. Phys. Chem. A* **1997**, *101*, 4121–4127.
- (27) For quadrupole echoes applied on macroscopic samples and coils, we used a static probe with a low-Q RF circuit so that we could use short excitation pulses of $1\mu\text{s}$. While this ensured small spectral distortions (as we verified by using large frequency offsets) we could not avoid the formation of significant Solomon echoes from multiple quantum transitions (powder sample). The latter interfere with recording of single quantum transition quadrupole echoes and lead to severe spectral distortions, unless we use long echo delays. Unfortunately, due to the spin echo decay most of the signal has decayed at sufficiently long delays so that the thus obtained spectra are compromised, as well. Nevertheless, within error, we find a similar featureless line shape as for the frequency stepped spin echoes, while we also ascertained that the small difference is not due to a bandwidth limitation.
- (28) Vleck, J. V. The Dipolar Broadening of Magnetic Resonance Lines in Crystals. *Phys. Rev.* **1948**, 116–1183.
- (29) Aikebaier, Y.; Kurosaki, K.; Sugahara, T.; Ohishi, Y.; Muta, H.; Yamanaka, S. High-

temperature thermoelectric properties of non-stoichiometric $\text{Ag}_{1-x}\text{InTe}_2$ with chalcopyrite structure. *Mater. Sci. Eng., B* **2012**, *122*, 999–1002.

(30) Van Kranendonk, J. Theory of quadrupolar nuclear spin-lattice relaxation. *Physica* **1954**, *20*, 781 – 800.

(31) Van Kranendonk, J.; Walker, M. Theory of quadrupolar nuclear spin-lattice relaxation due to anharmonic Raman phonon processes. *Phys. Rev. Lett.* **1967**, *18*, 701–703.

(32) Haase, J.; Oldfield, E. Spin-Echo Behavior of Nonintegral-Spin Quadrupolar Nuclei in Inorganic Solids. *J. Magn. Reson. Ser. A* **1993**, *101*, 30–40.